INSTITUTE OF PHYSICS PUBLISHING JOURNAL OF MICROMECHANICS AND MICROENGINEERING
J. Micromech. Microeng. **11** (2001) 270–276 www.iop.org/Journals/jm PII: S0960-1317(01)20518-X

Bubble-based micropump for electrically conducting liquids

X Geng[1], H Yuan[1], H N Oğuz[2] and A Prosperetti[1,2]

[1] Department of Mechanical Engineering, Johns Hopkins University, Baltimore, MD 21218, USA
[2] Department of Applied Physics, Twente Institute of Mechanics, Burgerscentrum, AE 7500 Enschede, The Netherlands

Received 5 January 2001

Abstract
This paper describes a novel pumping device without mechanical moving parts based on the periodic generation and collapse of a single vapour bubble in a channel. The channel shape is such that it creates an asymmetry in the surface tension forces, which results in a pumping effect. The principle can be implemented over a broad range of channel sizes and repetition frequencies. For illustration purposes, a particular implementation is described here where the working fluid is a salt solution in water, the channel diameters are of the order of 1 mm and the repetition frequency is between 1–10 Hz. In these conditions, the device develops a head of a few centimetres of water with typical flow rates in the range of 100 μl per minute. It appears possible to increase both head and flow rate by adjusting geometrical parameters and operating conditions. A simple modification of the design would render the same principle also applicable to the pumping of non-conducting liquids.

1. Introduction

Surface tension is a typical example of a force which is often negligible at conventional scales, but which becomes important, or even dominant, as the length scale is reduced. It is effects such as this which make the area of micromechanics both scientifically intriguing and technologically promising (see, for example, [1–5]).

In this paper, we describe a new pumping principle relying on surface tension and based on the periodic generation of a single vapour bubble in a suitably shaped channel. Although based on surface tension effects, the principle of operation is quite different from the Marangoni-induced flows used in other pumping devices (see, for example, [6–8]). Typically, in such devices, temperature differences are maintained along the bubble interface, which result in convective flow due to the dependence of surface tension on temperature (Marangoni flow). Here, on the other hand, the pumping effect is obtained by forcing different curvatures on different parts of the interface.

The implementation of the idea described here is applicable to electrically conducting liquids, but the modification mentioned in section 4 would make it possible to pump electrically non-conducting liquids as well. An advantage of this approach is the absence of valves or moving mechanical parts. On the negative side, a small fraction of the liquid to be pumped undergoes a significant temperature rise, which might make the device unsuitable for certain applications.

The device described here has a scale of several hundred micrometres, but the same principle appears capable of operating over a broad range of smaller and possibly somewhat larger scales as well. Variations and extensions are briefly mentioned in the final section.

The current literature contains many papers describing a variety of micropumps. A survey of the earlier ideas can be found, for example, in the reviews given in [1, 2, 9]; more recent work is described, among others, in [10–16]. The most widespread design involves a diaphragm, the actuation of which can be electrostatic, piezoelectric, or driven by phase change or other means. In many designs, the pumping action is obtained by coupling the diaphragm to suitable check valves, which requires a relatively complex fabrication process. The use of suitably shaped flow passages permits the avoidance of valves [10, 11], but this principle relies on inertial effects and may therefore not scale favourably as the pump size is reduced. A limitation common to all these pumps lies in the fact that the stroke provided by the diaphragm is typically small, and therefore so is the compression ratio. Among the disadvantages due to this feature is the fact that, if gas bubbles

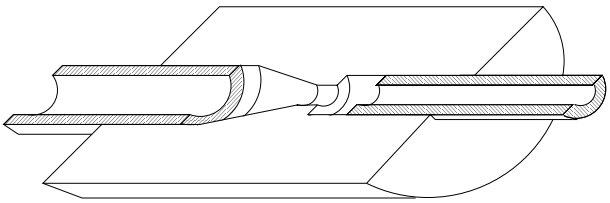

Figure 1. Sketch of one half of the pumping device cut by a plane through the axis of symmetry. In the implementation of the idea shown in figure 2, the pump material is plexiglas and the tubes are stainless steel needles.

remain entrapped in the pump or elsewhere in the hydraulic circuit, the functioning of the unit may be compromised even if efforts are made to decrease the dead volume [17]. A distinct characteristic of the system described in this paper is that the displacement provided by the pump can instead be quite large.

In addition to the ink-jet printer [18,19], the use of bubbles for micro-fluid applications has been considered before (see, for example, [4, 20–22]). However, the present paper differs from all these works in many aspects, as will be shown in the following material.

Although we discuss specific devices that have been built and tested in our laboratory, the primary objective of this paper is to describe the pumping principle which, as noted in the last section, appears capable of a variety of embodiments. This potential flexibility may make the idea suitable for a variety of applications such as electronic cooling, miniature chemical reactors, and others. Another promising aspect is that the first prototypes have already worked satisfactorily without any attempt at optimization. It may be expected therefore that a considerable scope exists for the improvement of effectiveness and reliability.

2. Description of the device

The crucial aspect of the principle on which the pumping action described in this paper is based is the shape of the flow passage in the neighbourhood of the location where the bubble is generated. For concreteness, in order to explain this point, we refer to one of the devices that we have built to date, and later on comment on the possible extensions and variations of the basic idea. Figure 1 shows one half of the device cut along a plane parallel to the direction of flow.

We start from a plexiglas cylinder with a diameter of 5 mm. Two coaxial holes are drilled in the cylinder (figure 1), one with a diameter of 1.6 mm, and the other with a diameter of 0.8 mm (the reason for using two different diameters will become apparent shortly). The two holes are joined by a short narrow passage—the throat—having a diameter of about 500 μm and a length of the same order. The flow passage between the throat and the larger tube has an approximately conical shape. Actual photographs of a prototype are shown in figure 2.

A 21-gauge stainless steel needle (outer diameter 813 μm, inner diameter 508 μm, wall thickness 152 μm) is inserted into the smaller hole and a 17-gauge stainless steel needle (outer diameter 1473 μm, inner diameter 1067 μm, wall thickness 203 μm) is inserted into the larger hole. The needles are connected to two reservoirs and the system is filled with a filtered saturated solution of table salt in water (density 1200 kg m^{-3}). When an ac voltage is applied between the two needles, the narrowing of the throat has the effect of locally increasing the current density in the water, which results in a strongly localized Joule heating and the generation of a vapour bubble. The voltage is maintained for a time τ, after which it is removed, causing the rapid condensation of the bubble. This cycle is repeated with a period $T \geqslant \tau$. We find experimentally that periods of the order of 100–1000 ms (i.e. frequencies of the order of 10–1 Hz) lead to a net pumping effect developing a steady head of the order of 2–3 cm of water. It should be stressed that, aside from a small amount of gas dissolved in the liquid, which diffuses into the bubble, the bubble consists essentially of vapour because the use of an ac current prevents the electrolytic evolution of any significant amount of free gas.

The important point is that the bubble's growth and collapse do not result in a vanishing net displacement of the liquid but, when averaged over a cycle, are capable of generating a pumping action in the direction of the wider channel. We begin with a description of the process, later developing a simple model.

Figure 2 shows a sequence of CCD-camera images of the bubble that forms under the conditions described for $\tau = 100$ ms and $T = 500$ ms. These images do not refer to a single bubble, but have been obtained with prescribed delays during subsequent events. This is possible in view of the repeatability of the phenomenon, that has been checked by high-speed video. We do not show images from the video sequences due to their lower quality. Figures 3(a) and 3(b) (the latter a detail of the former) show the current versus time for this case; the applied voltage was 46 V and the ac voltage frequency was 50 kHz. (Note that, as made clear by the expanded scale of figure 3(b), the small-scale 'scalloping' of the trace in figure 3(a) is not real, but only an artefact of the aliasing introduced by the digital oscilloscope.)

Initially, as the liquid heats up and its resistivity falls, the current grows. The first frame of figure 2, taken 3 ms after the start of the heating, shows a small vapour bubble in the narrow throat of the device. This bubble rapidly grows and the cross-sectional area available for electrical conduction decreases. The ensuing rapid increase in electrical resistance causes the current to fall. By this time, however, due to the large initial pressure and strong subsequent cooling of the vapour, the bubble has overshot its equilibrium volume and has over-expanded. This causes a partial collapse and a momentary increase of the current, which then settles to an approximately steady value as the bubble very slowly grows again. During this last phase, the current flows in a liquid film coating the wall. While this film, initially, is due to the viscous adherence of the liquid to the wall (the so-called no-slip condition), later on it is perhaps maintained by surface-tension driven flows. When the voltage is brought to zero at 100 ms, the current falls and the liquid rapidly cools. The vapour pressure correspondingly falls to a small value[1] and the bubble collapses to a very small residual size. This residual bubble is most probably filled with dissolved (and perhaps a small amount of electrolytically

[1] Recall that, even at a temperature as high as 50 °C, the saturated vapour pressure of pure water is only 12% of atmospheric pressure, while at 20 °C it is about 2%; in the presence of salt, the vapour pressure will be even lower.

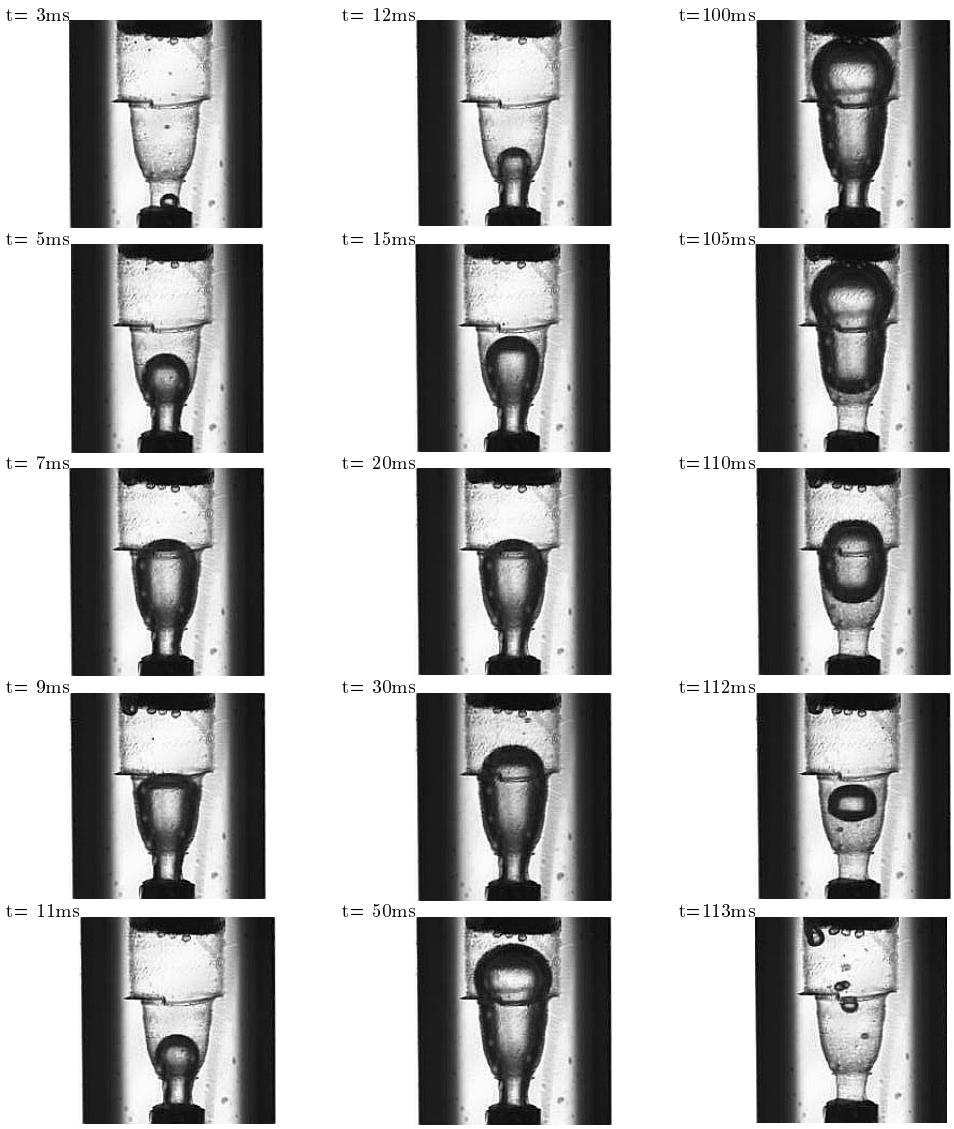

Figure 2. A sequence of CCD-camera images showing the bubble cycle. This sequence is formed from images acquired during different bubble cycles under nominally identical conditions. Note the uneven spacing of the images over the cycle. Gravity points down to the right. The heating time is $\tau = 100$ ms, the repetition rate is $T = 500$ ms, the applied voltage is 46 V, and the ac voltage frequency is 50 kHz. The black areas at the inlet and outlet of the device are the stainless steel needles serving also as electrodes.

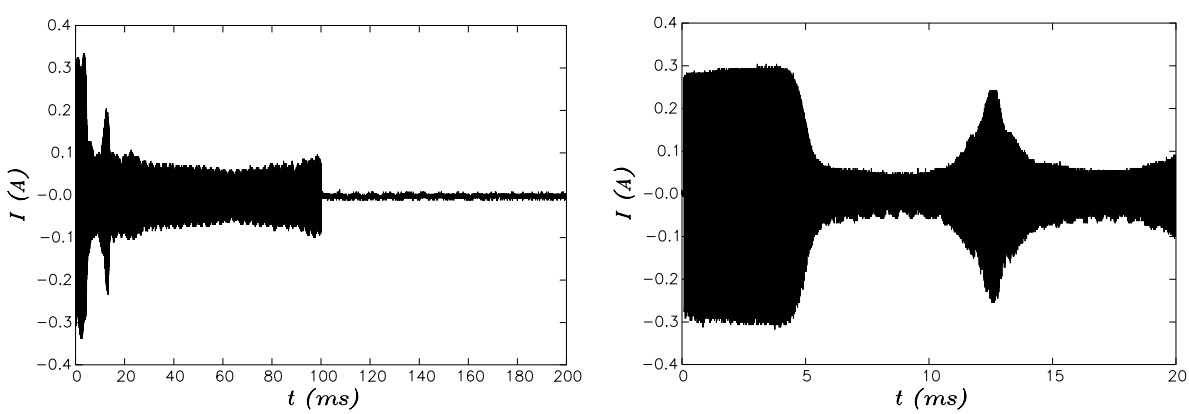

(*a*) (*b*)

Figure 3. (*a*) Current versus time for the case of figure 2. A voltage of 46 V is applied between 0–100 ms and the repetition time is 500 ms. As proven by its absence in figure 3(*b*) (which is a detail of figure 3(*a*)), the small-scale 'scalloping' of the trace is due to aliasing by the oscilloscope. (*b*) Detail of figure 3(*a*).

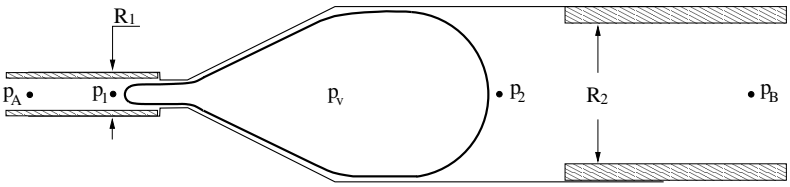

Figure 4. Sketch for the explanation of the principle of operation of the pump, see equation (4).

generated) gases that have diffused into the vapour volume during the previous growth process.

Joule heating using electrical currents with frequencies higher than the 50 kHz used in figures 3(*a*) and 3(*b*) gives rise to essentially the same phenomena, with the only difference that the residual gas bubble left behind by the collapsing vapour bubble is somewhat smaller.

It can be seen that, rather than near the point where the bubble originated, the final collapse occurs around a point located at some distance from the throat in the direction of the wider tube. This asymmetry between the upward moving liquid during growth and the more symmetric flow during collapse is the key feature responsible for the net pumping action. By orienting the pump in different ways with respect to gravity it is easily shown that this effect is not related to buoyancy.

The mechanism underlying the pumping action may be described as follows. Surface tension causes a pressure difference between the bubble interior and the surrounding liquid. Due to the fact that the lower tube is smaller than the upper one, the radius of curvature R_1 of the lower part of the bubble is smaller than the radius of curvature R_2 of the upper part (figure 4). With reference, for example, to the points on the axis of symmetry, we may write

$$p_v - p_1 = \frac{2\sigma}{R_1} \qquad p_v - p_2 = \frac{2\sigma}{R_2}, \tag{1}$$

where σ is the surface-tension coefficient and p_v is the vapour pressure in the bubble. Over the temperature range between 30–100 °C the surface tension of water changes by about 17% and therefore, even if there are temperature gradients along the bubble surface, this variation can be ignored as a first approximation. Furthermore, due to the small density of the vapour, the pressure inside the bubble can be assumed to be essentially uniform (see, for example, [23]). Thus, subtracting, we find from (1),

$$p_1 - p_2 = -2\sigma\left(\frac{1}{R_1} - \frac{1}{R_2}\right) < 0. \tag{2}$$

This relation shows that, in order to maintain equilibrium, the liquid pressure in the smaller tube upstream of the throat must be kept below the liquid pressure in the wider tube. In other words, there is a pressure increase in traversing the device from the narrow to the wide tube.

On this basis, we can construct a very simple bi-static model of the pump. Assume that the system can exist in two states, with and without the bubble. Let τ be the duration of the applied voltage. Due to the residual heat and inertia, the bubble lifetime is somewhat longer than τ, say by an amount Δt. Furthermore, we postulate that the pressure difference given by (2) exists whenever the bubble is present, and that we can take the radii R_1 and R_2 to equal the radius of the lower and upper tube, respectively. In this way, the time-averaged pressure difference developed by the pump becomes

$$\overline{p}_1 - \overline{p}_2 = -2\sigma\left(\frac{1}{R_1} - \frac{1}{R_2}\right)\frac{\tau + \Delta t}{T}, \tag{3}$$

where T is the repetition time (e.g. 500 ms for the example of figures 3(*a*) and3(*b*)) and the overline denotes the time average.

With this relation we can express the difference $\Delta p = p_B - p_A$ between the time-averaged pressures p_A and p_B at the inlet and outlet of the system (figure 4):

$$\begin{aligned}\Delta p &= (p_B - p_2) + (p_2 - p_1) + (p_1 - p_A) \\ &= (p_B - p_2) + (p_1 - p_A) + 2\sigma\left(\frac{1}{R_1} - \frac{1}{R_2}\right)\frac{\tau + \Delta t}{T},\end{aligned} \tag{4}$$

where all pressures are to be understood in a time-averaged sense. In the absence of gravity and flow, on average, $p_B = p_2$, $p_A = p_1$ and, therefore, $\Delta p > 0$ or $p_B > p_A$. In other words, in order to maintain the condition of zero net flow assumed in the calculation, it is necessary to apply a sufficiently large adverse pressure differential. If p_B is not large enough, there will therefore be a flow from the lower to the higher pressure, i.e. the system will operate as a pump.

This argument is true if $p_B - p_2$, $p_A - p_2$ are negligible, which is the case at low frequencies when inertia is small. At higher frequencies, these pressure differences will depend on the length of the liquid columns and flow resistances and the pump may become less effective or even invert the flow direction. For instance, we have found that, if the voltage is shut off when the current first falls (i.e. about 6 ms for the case of figures 2 and 3), although very reproducible, the bubble remains always small with a short lifetime and little or no pumping takes place. When inertial effects are even greater, the behaviour of the system changes qualitatively and the pumping effect becomes inertia-controlled. We have studied this situation in a recent paper [24].

A sketch of the experimental set-up is shown in figure 5. A PC controls a function generator, which powers the pump via an amplifier, the strobe, and the CCD camera. The inlet and outlet of the pump are connected by 0.13 m long silicon tubes to two beakers, one of which can be raised by an accurately measurable amount. The inlet tube had a diameter of 0.79 mm and the outlet tube of 1.58 mm. The flow rate was measured by monitoring the displacement of an air bubble blocking the outlet tube.

3. Results

In order to interpret in a very preliminary way the results of the measurements, we use the simple relation (3) derived

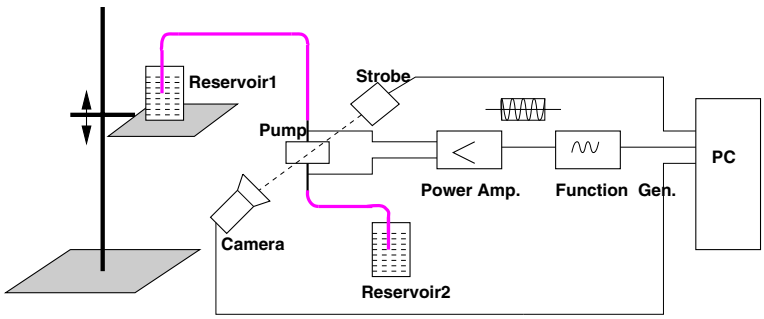

Figure 5. Sketch of the arrangement used in the experiment. A PC controls a function generator (which powers the pump via an amplifier), the strobe, and the CCD camera. The inlet and outlet of the pump are connected by silicon tubes to two beakers one of which can be raised by an accurately measurable amount.

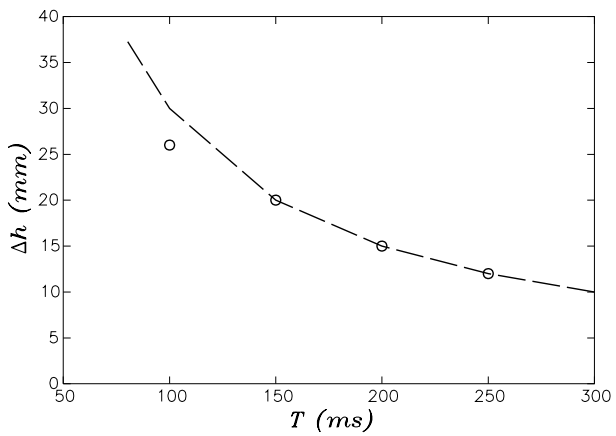

Figure 6. Zero-flow-rate head (in mm of saturated salt water; 1 mm_{H_2O} = 11.8 Pa) as a function of the repetition period T for a fixed heating time τ = 50 ms and a voltage of 46 V. The symbols represent the data and the dashed line is the prediction (3) calculated for Δt = 30 ms.

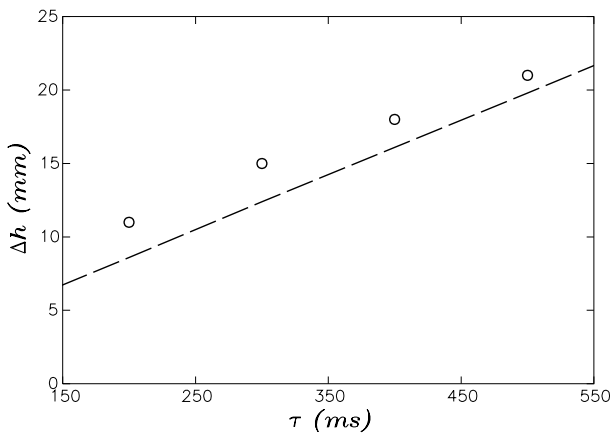

Figure 7. Zero-flow-rate head (in mm of saturated salt water; 1 mm_{H_2O} = 11.8 Pa) as a function of the heating time τ for fixed repetition period T = 1000 ms and a voltage of 46 V. The symbols represent the data and the dashed line is the prediction (3) calculated for Δt = 30 ms.

earlier. As mentioned before, we assume the bubble to last longer than the heating time τ by an amount Δt. This time interval accounts for the finite rate of heat dissipation and the fact that the bubble growth and collapse are not instantaneous. As far as heat dissipation is concerned, one may argue that, provided that steady state has been reached during the heating phase (i.e. τ is long enough), the rate at which heat is removed when the current is interrupted is approximately independent of the duration of the heating. This is so because the maximum temperatures reached are determined by the ambient pressure and therefore will be of the order of 100 °C, independent of the duration of heating. If it were otherwise, the bubble behaviour during the heating period would be very dynamic, contrary to observation. The other factor that influences Δt is the finite rate of growth and collapse of the bubble. Since the bubble dynamics is governed by the difference between the vapour pressure and the ambient pressure, and since this difference, for the reason mentioned before, is approximately constant, one may expect Δt to be approximately constant or, at any rate, to vary slowly with the control parameters τ and T. Thus, we propose to adjust Δt so as to fit one experiment, and to examine the model predictions for other cases keeping it constant. For the results reported the applied voltage was 46 V.

Figure 6 shows the zero-flow-rate head (measured in mm of water, with a density of 1200 kg m^{-3} due to the addition of salt; 1 mm_{H_2O} = 11.8 Pa) as a function of the repetition period T for a fixed heating time τ = 50 ms; Δt is determined by fitting the theoretical line of (3) to the last point (T = 250 ms), and is found to have a value of 30 ms. The symbols represent the data and the dashed line is the prediction (3). There is some uncertainty as to the best value of σ to use due to the time dependence of the bubble surface temperature. Here, and in the following, we take an intermediate value of 68 dynes/cm noting that, in view of the approximate nature of the model, one is more interested in trends than in precise numerical values. The simple model previously described is clearly inapplicable when $T < \tau + \Delta t$, which equals 80 ms in this case; for this reason we only show the theoretical prediction for $T \geqslant \tau + \Delta t$. When T is close to $\tau + \Delta t$, a bubble is essentially present all the time and the predicted Δp is close to the negative of the value given by (2). For the 46 V applied here, however, experimentally the system is found to be rather unstable in this parameter range.

Figure 7 shows the measured zero-flow-rate head as a function of the heating time τ for fixed T = 1000 ms and, again, Δt = 30 ms. The predicted linear behaviour is fairly well supported by the data. As τ increases, the time available for the removal of the heat decreases and the functioning of the pump becomes somewhat less regular. We have observed that,

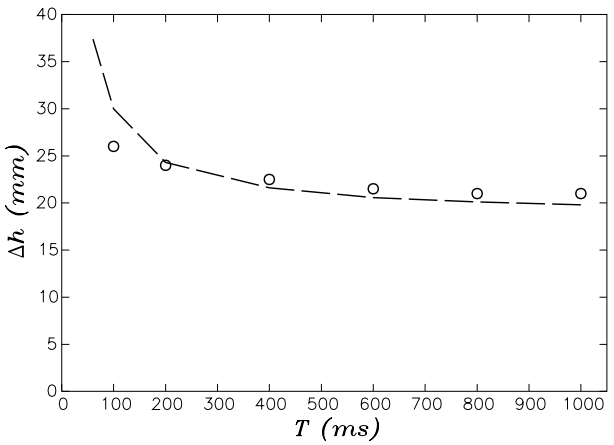

Figure 8. Zero-flow-rate head (in mm of saturated salt water; 1 mm_{H_2O} = 11.8 Pa) as a function of the repetition period T for a constant fraction of the heating time, τ/T = 1/2; the applied voltage is 46 V. The symbols represent the data and the dashed line is the prediction (3) calculated for Δt = 30 ms.

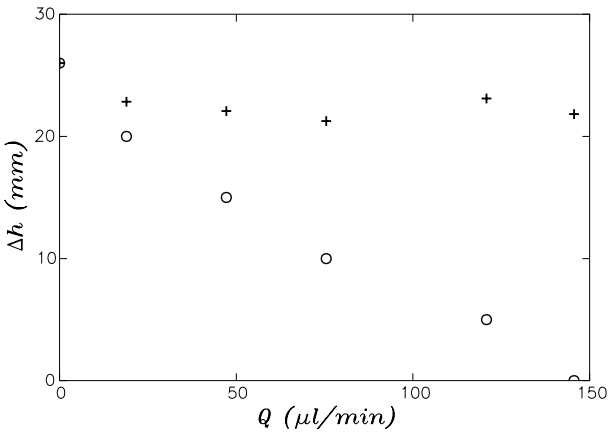

Figure 9. Measured head (in mm of saturated salt water, circles; 1 mm_{H_2O} = 11.8 Pa) versus flow rate through the pump set-up for a repetition period T = 100 ms, a heating time τ = 50 ms, and an applied voltage of 46 V. In order to compensate for the effect of the tubing and other flow resistances, the head necessary to produce the same flow rate was also measured with the pump shut off. The data marked by crosses are obtained by adding the pressure drops measured in this way to the data represented by the circles. These data are therefore a better representation of the net pumping head.

for voltages of 40 V or higher applied nearly continuously, the volume of the vapour space fluctuates: a bigger bubble limits the current, which causes a partial condensation, a consequent reduction of electrical resistance, more heating, a growing bubble etc. This cycle repeats irregularly, but the net effect is an effective bubble lifetime shorter than the estimate $\tau + \Delta t$. This accounts for the slight downward trend of the data when τ is large.

Figure 8 is similar, but here the zero-flow-rate head is measured as a function of the period T keeping the fraction τ/T of the heating time constant and equal to 1/2 (again with Δt = 30 ms). When the period is very short, the rapidly supplied heat does not have time to diffuse away. Bubbles do not completely collapse in between heating periods and interfere with the current supply during the following cycle. In these conditions the functioning of the device is rather irregular. As the heating time increases with the period, however, the effect of Δt is immaterial and both theory (equation (3)) and data converge to

$$2\sigma\left(\frac{1}{R_1}-\frac{1}{R_2}\right)\frac{\tau}{T}, \tag{5}$$

which, in the present case, is approximately 20 mm of water.

Finally, in figure 9, we show data of head versus flow rate for T = 100 ms and τ = 50 ms. As noted in connection with the previous figure, these parameter values give rise to a somewhat irregular behaviour at zero flow rate, but not so when there is enough convection through the pump to dissipate heat. The circles show the measured heads, which include the flow resistance of the tubing and other flow passages. In order to remove the effect of these factors, the head necessary to produce the same flow rate was also measured with the pump shut off. By adding these values to the circles, we find the values marked by crosses that are a better estimate of the head generated by the pump alone. These data indicate that the pump head is essentially independent of flow rate except possibly for Q = 0, where the heat removal is inefficient.

It may be noted that the measured pumping rate through the apparatus (circles in figure 9) is of the same order as in other pumping devices with mechanical moving parts (see, for example, [2]). However it should also be stressed that, as noted before, we have made no attempt to optimize the micropump described here.

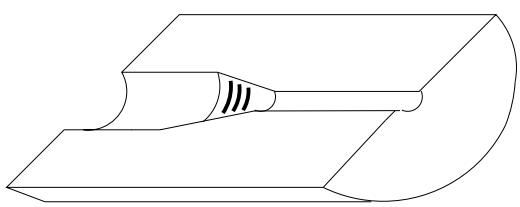

Figure 10. Sketch of a variant of the pump of figure 1 suitable for use with non-conducting liquids. The black stripes in the conical region represent the heater used to generate the bubble.

4. Conclusions and outlook

The purpose of this paper was to present the general principle and some preliminary results on what we believe to be a potentially useful pumping device without moving mechanical parts. In spite of its preliminary nature, this work suggests that the device offers potential for development and optimization.

Although the implementation that we have described is only useful for electrically conducting liquids, the same principle can be used for dielectric liquids if the bubble is generated by a heater embedded in the wall (figure 10). In this case, there would be no need for metal needles or a throat, and the bubble would be generated by positioning a heater in the conical region.

Other improvements can be achieved by the use of more sophisticated techniques to shape the flow passages, with different materials and procedures. For instance, silicon microfabrication can produce small flow passages and accurately shaped heaters. The interest in smaller ducts, of course, lies in the greater head that can thereby be generated due to surface tension. This increase in head would be

obtained at the expense of an increased flow resistance, which could however be limited by using bigger conduits everywhere except at the pump itself, or even several pumps in parallel. A square or moderately rectangular shape of the cross section of the flow passages (such as would be produced by standard silicon microfabrication techniques) would not be expected to change the behaviour of the system in a qualitative way [25–27]. Differences in the thermal conductivity of the solid materials (e.g. silicon versus plexiglas), would lead to differences in the bubble lifetime, which could however be compensated by altering the heating parameters. An analysis of the heat transfer processes in a related device has been presented in a recent paper [28].

Many small pumps can also be connected in series similarly to the situation studied in [24]. Small embedded thermocouples, with or without a control loop, would allow a real-time precise control of the bubble generation cycle and, thereby, of the pumping action.

Acknowledgments

This study has been supported by AFOSR under grant F49620-96-1-0386 and by NSF under grant CTS-9989965.

References

[1] Gravesen P, Branebjerg J and Jensen O S 1993 Microfluidics—a review *J. Micromech. Microeng.* **3** 168–82

[2] Elwenspoek M, Lammerink T S J, Miyakei R and Fluitman J H J 1994 Towards integrated microliquid handling systems *J. Micromech. Microeng.* **4** 227–45

[3] Gad-el Hak M 1999 The fluid mechanics of microdevices *J. Fluids Eng.* **121** 5–33

[4] Lin L, Pisano A P and Carey V P 1998 Thermal bubble formation on polysilicon resistors *J. Heat Transfer* **120** 735–42

[5] Detlefs W *et al* January 1999 *MicroElectroMechanical Systems (MEMS)—An SPC Market Study* (System Planning Corporation, 1429 North Quincy Street, Arlington, VA 22207, USA)

[6] Takahashi K, Weng J G and Tien C L 1999 Marangoni effect in microbubble systems *Microscale Thermophys. Eng.* **3** 169–82

[7] Debar M and Liepmann D 2000 Steady-state microscale pumping using the Marangoni effect: A model problem *Bull. Am. Phys. Soc.* **45** 126

[8] Liepmann D and Debar M 2000 Development of a microfabricated single-bubble pump *Bull. Am. Phys. Soc.* **45** 137

[9] Shoji S and Esashi M 1994 Microflow devices and systems *J. Micromech. Microeng.* **4** 157–71

[10] Olsson A, Stemme G and Stemme E 1999 A numerical design study of the valveless diffuser pump using a lumped-mass model *J. Micromech. Microeng.* **9** 34–44

[11] Jiang X N, Zhou Z Y, Huang X Y, Li Y, Yang Y and Liu C Y 1998 Micronozzle/diffuser flow and its application in micro valveless pumps *Sensors Actuators* A **70** 81–7

[12] Nguyen N T, Schubert S, Richter S and Dötzel W 1998 Hybrid-assembled micro dosing system using silicon-based micropump/valve and mass flow sensor *Sensors Actuators* A **69** 85–91

[13] Français O and Dufuour I 1998 Dynamic simulation of an electrostatic pump with pull-in and hysterisis phenomena *Sensors Actuators* A **70** 56–60

[14] Koch M, Harris N, Evans A G R, White N M and Brunnschweiler A 1998 A novel micromachined pump based on thick-film piezoelectric actuation *Sensors Actuators* A **70** 98–103

[15] Acero M C, Plaza J A, Esteve J, Carmona M, Marco S and Samitier J 1997 Design of a modular micropump based on anodic bonding *J. Micromech. Microeng.* **7** 179–82

[16] Zengerle R, Ulrich J, Kluge S, Richter M and Richter A 1995 A bidirectional silicon micropump *Sensors Actuators* A **50** 81–6

[17] Richter M, Linnemann R and Woias P 1998 Robust design of gas and liquid micropumps *Sensors Actuators* A **68** 480–6

[18] Asai A, Hara T and Endo I 1987 One-dimensional model of bubble growth and liquid flow in bubble jet printers *Japan. J. Appl. Phys.* **26** 1794–801

[19] Asai A 1989 Application of the nucleation theory to the design of bubble jet printers *Japan. J. Appl. Phys.* **28** 909–15

[20] Lin L and Pisano A P 1991 Bubble forming on a micro line heater *Micromechanical Sensors, Actuators, and Systems, DSC* vol 32, ed D Cho (ASME) pp 147–63

[21] Lin L, Udell K S and Pisano A P 1994 Liquid-vapor phase transition and bubble formation in microstructures *Thermal Sci. Eng.* **2** 52–9

[22] Jun T K and Kim C J 1996 Microscale pumping with traversing bubbles in microchannels *Solid-State Sensor and Actuator Workshop (Hilton Head Island, June 1996)* Transducer Research Foundation 96TRF-0001, pp 144–7

[23] Hao Y and Prosperetti A 1999 The dynamics of vapor bubbles in acoustic pressure fields *Phys. Fluids* **11** 2008–19

[24] Yuan H and Prosperetti A 1999 The pumping effect of growing and collapsing bubbles in a tube *J. Micromech. Microeng.* **9** 402–13

[25] Wong H, Radke C J and Morris S 1995 The motion of long bubbles in polygonal capillaries: Part 1. Thin films *J. Fluid Mech.* **292** 71–94

[26] Wong H, Radke C J and Morris S 1995 The motion of long bubbles in polygonal capillaries: Part 2. Drag, fluid pressure and fluid flow *J. Fluid Mech.* **292** 95–110

[27] De Lazzer A and Langbein D 1998 Liquid surface in regular N-pods *J. Fluid Mech.* **358** 203–21

[28] Yuan H, Oğuz H N and Prosperetti A 1999 Growth and collapse of a vapor bubble in a small tube *Int. J. Heat Mass Transfer* **42** 3643–57